Adsorption Efficiency of Fe(III) from Solution by Zeolite Y Synthesized from Rice Husk

Sittichai Kulawong[1]* and Jittima Kulawong[2]

[1]Program of Chemistry, Faculty of Science and Technology, Nakhon Ratchasima Rajabhat University, Nakhon Ratchasima 30000, Thailand

[2]Faculty of Engineering, Vongchavalitkul University, Nakhon Ratchasima 30000, Thailand

* Corresponding author. E-mail address: sittichai_kul@hotmail.com

Abstract

The purposes of this work were to prepare zeolite Y in sodium form (NaY) by using silica from rice husk, and to test the adsorption efficiency of the prepared NaY. The NaY was characterized by x-ray diffraction (XRD) and Brunauer, Emmett and Teller (BET) to confirm their structures and properties including isotherm adsorption and surface area. In addition, the adsorption efficiency of the NaY was tested in Fe(III) solution. The adsorption characteristics, contact time, initial concentration of iron solution, pH, and amount of adsorbent on the NaY, were studied. The time taken to reach equilibrium was 30 min. The amount of iron solution adsorbed increased as the pH increased, and the optimum values were pH 4.0-6.0. The adsorption capacity of the iron species in a solution at 30 °C was 57.80 mg/g, at 40 °C, 90.91 mg/g, and at 50 °C, 60.61 mg/g. The isotherms and isotherm constants were depicted from the results of the Langmuir and Freundlich adsorption. Adsorption isotherm data of the Fe(III) solution, when tested at 30 °C, could be well explained by the Langmuir model but that of Fe (III) tested at 40 °C and 50 °C were more related to the Freundlich model. The positive enthalpy ($\Delta H°$) and the negative Gibbs free energy ($\Delta G°$) suggested that the process of adsorption of the iron solution on the NaY was endothermic and spontaneous. The study of the kinetic adsorption model correlated with the pseudo-second order.

Keywords: zeolite, adsorption, iron, rice husk

Introduction

Zeolites are crystalline aluminosilicates consisting of tetrahedral TO_4 units (T=Si or Al) bonded together by sharing oxygen atoms and the balanced charge of the extra-framework with metal cations (M^+). The zeolites had specific size, shape and channel, with well-defined porous structures. Their porosity was classified as microporous material, less than 2.0 nm (Wittayakun, Khemthong, & Prayoonpokarach, 2008). These dominant properties are beneficial for several applications, such as an adsorbent in wastewater containing organic and inorganic pollutants, ion-exchange capability and catalyst support (Osakoo et al., 2017; Kulawong, Prayoonpokarach, Neramittagapong, & Wittayakun, 2011; Rakmae et al., 2016). Zeolites are widely used as heterogeneous catalysts (catalyst and support), and are one of the most used applications in the various of industrial chemical reactions such as petroleum cracking, isomerization and alkylation reactions due to their mechanical strength, thermal stability, high-pressure resistance and easy to separate from products (Wittayakun & Grisdanurak, 2004).

The zeolites, when used as catalysts, are mostly added with various types of transition metals, rich electrons in d orbital such as platinum (Pt), copper (Cu) and iron (Fe). Those metals are mostly transformed into cationic form and act as promoters to enhance the performance of the support and/or active sites such as Fe/ZSM-5, Fe/MCM-41, Fe/MCM-48, Fe/MOR and Fe/NaY. (Kulawong, Prayoonpokarach, Neramittagapong, & Wittayakun, 2011; Wantala et al., 2010; Choi, Yoon, Jang, & Ahn, 2006; Park et al.,

2006; Villa, Caro, & de Correa, 2005; Zhao, Luo, Deng, & Li, 2001). These catalysts have been tested for phenol hydroxylation, which is a reaction between phenol (C_6H_5OH) and hydrogen peroxide (H_2O_2) to produce two benzenediols ($C_6H_4(OH)_2$) including catechol and hydroquinone. These products can be applied in many applications including photographic chemicals, antioxidants, polymerization inhibitors, and others (Brook et al., 1982). The conversion rate of phenol and the selectivity of the products compared with the reaction time were different depending on the pore size, surface area of the zeolites and the amount of Fe loading. However, the catalysts were slightly deactivated with times increased probably due to coke formation caused by covering and/or blocking of carbon on the surface of the zeolites (Kulawong, Prayoonpokarach, Neramittagapong, & Wittayakun, 2011; Kosri et al., 2017). Alternately, processing at a high temperature could affect metal sintering, resulting in a larger metal size and lower metal dispersion (Mäki-Arvela & Murzin, 2013). To minimize these problems, the catalyst has to be prepared by a suitable method, depending on the specific properties of each zeolite.

The properties of the catalyst depend on the process utilized in the preparation. Thus, the preparation step should take into account the physical properties of each zeolite, such as surface area, stability and durability. An efficient preparation method generates a strong interaction between the metal and the zeolite, resulting in a good metal dispersion, reduced catalyst sintering and an increase in the activity at the active sites (Rakmae et al., 2016). One of the most widely used methods in the preparation of supported catalysts on zeolites is the adsorption or ion-exchange resulting from the zeolites becoming negatively charged, higher than their point of zero charge (PZC), when they are dispersed into solution. The consequence was favorable to interact with the metal in cation form, dissolving in a solution (Mäki-Arvela & Murzin, 2013).

There have been reports that rice husks are composed of 60-70% hydrocarbon compounds, 20-30% silica, together with small amounts of metal oxides and heavy metals (Wittayakun, Khemthong, & Prayoonpokarach, 2008; Johar, Ahmad, & Dufresne, 2012). The silica purity from the rice husks could be improved by acid leaching to remove impurities and calcination in air to eliminate organic components. The purity of the silica processed in this way was up to 98-99%, which makes it suitable as a raw material for the synthesis of zeolites (Real, Alcala, & Criado, 1996). Thus, our work, silica from rice husk was used to synthesize NaY zeolite. Then, the phase structure and surface properties of the NaY zeolite were studied by x-ray diffraction (XRD) and nitrogen adsorption-desorption. The NaY zeolites were then tested for absorption of Fe(III) from solution. To search the best conditions for the preparation of the Fe catalyst supported on the NaY, the effects of temperature, absorption time and pH were varied and investigated. Finally, isotherm and kinetic absorption of the Fe were also studied.

Methods and Materials

Chemicals

Hydrochloric acid (37% HCl, Carlo Erba), potassium hydroxide (99% KOH, Carlo Erba), Sodium hydroxide (99 % NaOH, Carlo Erba), Sodium aluminate (Na 50-56 % and Al 40-45 %; $NaAlO_2$, Riedel-de Haën®) and iron (Fe) (prepared from 99% $FeCl_3 \cdot 6H_2O$, QRëC).

Experimental

1. Preparation of silica from rice husk

Silica from rice husk was prepared by refluxing the rice husks in 3 M HCl at 80 °C for 3 h (the ratio of rice husk to acid of 1:1); a process adapted from the work of Kulawong and coworkers (2011). Then, the silica was washed with distilled water until the solution was neutral, dried and calcined at 600°C for 6 h.

2. Preparation of sodium silicate

28.7 g of the silica prepared from the rice husk was dissolved in 14% w/w of NaOH (100 mL), then stirred for 24 h and filtered. Sodium silicate with the ratio of 28.7% SiO_2 and 8.9% Na_2O, was obtained.

3. Synthesis of NaY zeolite

NaY zeolite was synthesized from a seed gel and feedstock gel by a method adapted from Ginter and coworkers (1992). The seed gel with a molar ratio of $10.67Na_2O$: Al_2O_3:$10SiO_2$:$180H_2O$ was prepared by dissolving NaOH (4.07 g) and $NaAlO_2$ (2.9 g) in distilled water (19.95 g). The mixture was then slowly added with $NaAlO_2$ (22.27 g), which was stirred for 30 min and then transferred into a polypropylene (PP) bottle, capped, and aged at ambient temperature for 24 h. The aged feedstock gel with molar ratio $4.30Na_2O$: Al_2O_3:$10SiO_2$:$180H_2O$ was prepared by dissolving NaOH (1.40 g) and $NaAlO_2$ (13.09 g) in distilled water (130.97 g). The mixture was then slowly added with $NaAlO_2$ (142.43 g), stirred for 30 min and used immediately without aging by adding to the seed gel (16.50 g) under stirring. The final mixture consisted of a molar ratio of $4.62Na_2O$: Al_2O_3: $10SiO_2$: $180H_2O$. The final step was to transfer the mixture to a PP bottle, capped, and crystallized at 100 °C for 12 h, and the solid product was washed with DI water several times, filtered and dried at 80 °C for 24 h. It was then further characterized by XRD and BET.

4. Characterization of NaY zeolite

The NaY zeolite was analyzed by XRD (Bruker AXS diffractometer D5005) using Ni filtered Cu $K\alpha$ radiation. Their surface area, pore volumes and pore sizes were determined by nitrogen adsorption-desorption analysis (Micromeritics ASAP 2010). Before the measurement, each sample was degassed under vacuum at 300 °C. The surface area was calculated by Brunauer, Emmett and Teller method (BET) with relative pressure from 0.02 to 0.20.

5. Adsorption of Fe(III) in aqueous solution

5.1. Preparation of adsorbent (NaY zeolite)

The NaY zeolite was dried at 105°C for 12 h in an oven, then sieved to a desired particle size, and then kept in desiccator.

5.2. Effect of initial Fe(III) concentration and contact time.

Fe(III) solutions with a concentration of 30.00, 60.00, 90.00, and 120.00 mg/L were prepared by dissolving $FeCl_3 \cdot 6H_2O$ precursor in distilled water and adjusting the volume of the solution to 50 mL. The pH of each solution was adjusted to 5.00 by adding a solution of NaOH (0.10 M). The prepared solution was then shaken at a constant speed of 150 rpm at 30 °C for 60 min, and then the NaY zeolite (0.1 g) was added to each prepared solution and the mixture solution was continuously shaken for 5 min, and filtered to separate the adsorbent from the mixture. The amount of Fe(III) remaining in a solution was measured using a UV-visible light spectrophotometer at 471 nm. The contact time of each measurement was varied for 5, 10, 15, 30, 60, 90, 120 and 150 min.

5.3. Optimization of NaY zeolite content

Fe(III) solution with a concentration of 90.00 (mg/L) was prepared using the method described in 5.2, and seven 250 mL volumetric flasks were filled with the prepared solution. A different amount of NaY zeolite (0.02, 0.04, 0.06, 0.08, 0.10, 0.12 and 0.14 g) was added into each flask, and the flasks were continuously shaken for 30 min, then the solutions were filtered to separate the adsorbent from the mixture. The amount of Fe(III) remaining in each solution was measured by using a UV-visible light spectrophotometer at 471 nm.

5.4. Effect of pH on Fe(III) adsorption

Fe(III) solution with a concentration of 90.00 (mg/L) was prepared using the method described in 5.2, and then transferred into seven 250 mL volumetric flasks. A solution of NaOH (0.10 M) and HCl (0.10 M) were then added to the Fe(III) solution in each flask to adjust the pH in the flask to 2.00, 3.00, 4.00, 5.00, 6.00, 7.00 and 9.00. NaY zeolite (0.1 g) was then added to each flask which was shaken at 30 °C for 60 min, then filtered to separate the adsorbent from the mixture. The amount of Fe(III) remaining in solution was measured by using a UV-visible light spectrophotometer at 471 nm.

5.5. Adsorption isotherm

Fe(III) solutions with concentrations of 20.00, 30.00, 40.00, 50.00, 60.00, 70.00, 80.00, 90.00 and 100.00 (mg/L) were prepared and the pH adjusted using the method described in 5.2. NaY zeolite (0.1 g) was added into each flask which was shaken at 30 °C for 60 min, then the solutions filtered to separate the adsorbent from the mixture. The amount of Fe(III) remaining in solution was measured by using a UV-visible light spectrophotometer at 471 nm. The measurement was done twice with a similar procedure but at different temperatures of 40 °C and 50 °C.

Results and discussion

Characterization of NaY zeolite

Phase, crystallinity, sorption properties and BET surface area of the NaY zeolite were characterized by XRD and nitrogen adsorption-desorption. The XRD and nitrogen adsorption-desorption results of the NaY zeolite were reported in our previous work (Kulawong & Kulawong, 2017). Characteristic peaks of the NaY zeolite were observed at 6, 10, 16, 23 and 31 degrees and adsorption isotherm of that zeolite was type (I) attributing to a characteristic isotherm of microporous materials. Its BET surface area was 866 m^2/g. Moreover, the adsorption of nitrogen was quickly at lower relative pressure and became nearly constant due to a monolayer formation (Osakoo et al., 2017; Bunmai et al., 2018).

Effect of initial Fe(III) concentration and contact time

Percentage removal and adsorption capacity of Fe(III) measured at equilibrium were calculated according to equations (1) and (2).

$$\% \text{ removal} = \left(\frac{C_0 - C_e}{C_0} \right) \times 100 \quad (1)$$

$$q_e = \left(\frac{C_0 - C_e}{W} \right) \times V \quad (2)$$

Where C_0 (mg/L) is the initial Fe(III) concentration, C_e (mg/L) is the concentration of Fe(III) at equilibrium, q_e (mg/g) is the equilibrium adsorption capacity of Fe(III) adsorbed on unit mass of NaY zeolite, W (g) is the weight of NaY zeolite and V (L) is the volume of Fe(III) solution.

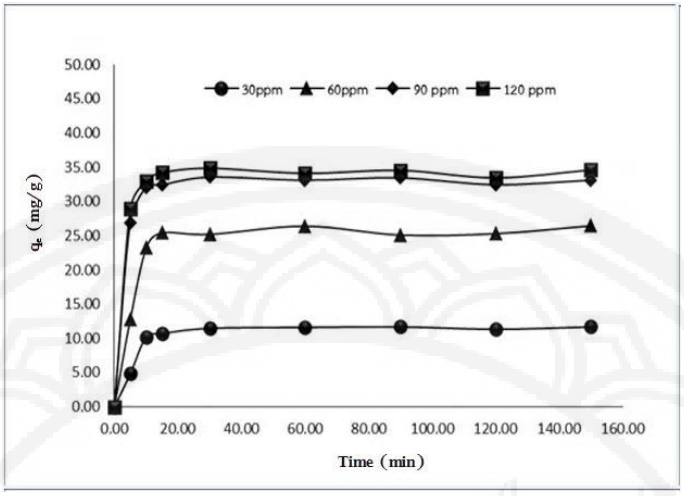

Figure 1 Adsorption capacity on various initial concentrations as a function of time (min)

Figure 1 shows the adsorption capacity of Fe(III), at various initial concentrations as a function of contact time (min). The results suggested that the adsorption rate of the Fe(III) was quickly adsorbed on the surface of the adsorbent at the start of the process due to an availability of adsorption sites and then the adsorption rate of the Fe(III) became constant, reaching to equilibrium after 30 min (Wang, Zhang, Zhao, Li, & Zhang, 2010), as the adsorption sites were occupied. The adsorption capacity of the Fe(III) increased as the concentrations of the Fe(III) increased as follows: 11.46, 25.20, 33.45 and 34.55 (mg/g) according to the increase of propulsion or mass transfer. However, the adsorption capacity of Fe(III) slightly improved when the concentrations increased from 90.00 (mg/L) to 120 (mg/L) because of a reaching to saturated concentrations. Thus, the initial concentration of Fe(III) solution at 90.00 (mg/L) was chosen for further study of the effect of adsorbent amount and pH for the Fe(III) adsorption. As a comparison, Hashemain and coworkers (2013) reported that the lapsed time from initial contact to equilibrium was 90 min, and the adsorption capacity of Fe ion at saturated concentration on Linde Type-A zeolite (0.1 g) were 90 min and 70 mg/L. Therefore, our work, those parameters based on surface area and porosity of the NaY zeolite for the Fe(III) adsorption were greater than the Linde Type-A zeolite owing to a shorter time to equilibrium and a larger concentration taken.

Optimization of NaY zeolite content

Figure 2 illustrates the adsorption capacity of the Fe(III) as a function of NaY zeolite content, which ranged from 0.02 g to 0.14 g. The adsorption capacity of the Fe(III) enhanced by the amount of the NaY zeolite due to the increased number of adsorption sites. The adsorption efficiency was slightly enlarged, when the amount of adsorbent increased to 0.1 g due to the overlapping of active sites at higher mass of the adsorbents (Seliem & Komarneni, 2016). Thus, the NaY zeolite (0.1 g) was a suitable quantity for the Fe(III) adsorption and selected for further study.

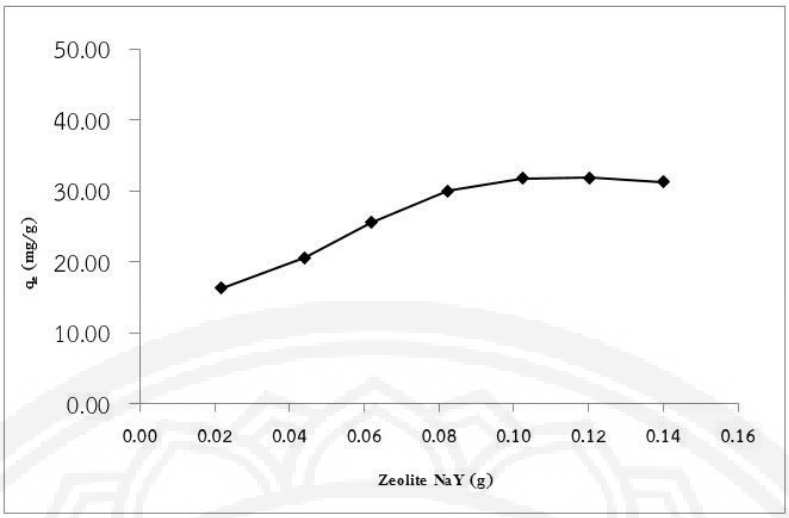

Figure 2 Adsorption capacity of Fe (III) as a function of NaY zeolite content (g)

Effect of pH on Fe(III) adsorption

Figure 3 demonstrates the effect of pH on Fe(III) adsorption. The adsorption capacity increased as the pH of the Fe(III) solution increased from 2.0 to 5.0, with the optimum point being around pH 4.0-6.0. Then, the adsorption efficiency of the Fe(III) solution decreased as the pH decreased from 6.0 to 9.0. The lower adsorption capacity at pH 2.0 and 3.0 could be from the competitive adsorption between H^+ and Fe(III) on the surface of the NaY zeolite. In contrast, the lower adsorption capacity at pH 7.0 and 9.0 was due to the precipitation of Fe(III) to mainly $Fe(OH)_3$ species, which is rarely soluble in water. The small amount of adsorption observed with the increase in pH from 7.0 to 9.0 was probably due to the presence of other ion species, $Fe(OH)_2^+$ and $Fe(OH)_4^-$, which is in good agreement with the report from Deng and coworkers (2017).

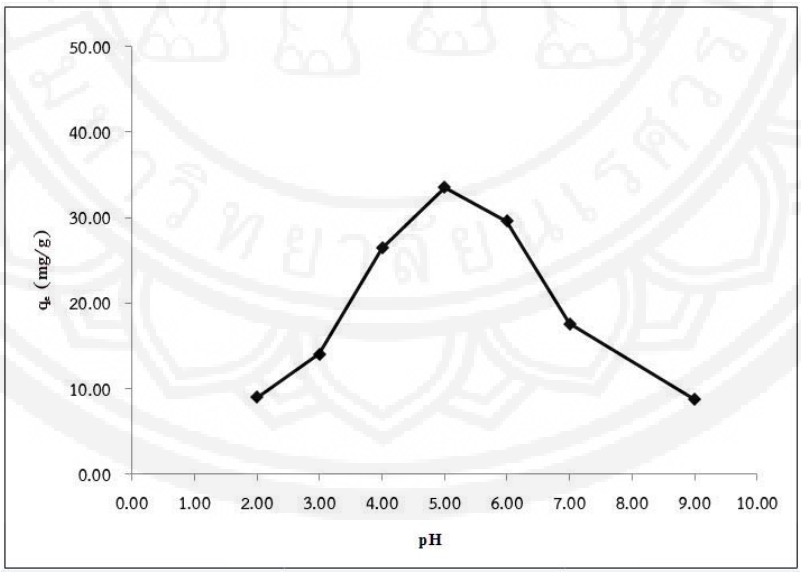

Figure 3 Effect of pH on adsorption capacity

Adsorption isotherm

The influence of temperature on the adsorption isotherm, from 30 to 50 °C, was studied. The data obtained was evaluated to identify the correlation between the concentration of the Fe(III) at equilibrium and the equilibrium adsorption capacity of the Fe(III) adsorbed in unit mass of NaY zeolite by using Freundlich and Langmiur isotherm models as follows: equations (3) and (4).

$$\ln(q_e) = \ln(K_F) + 1/n \ln(C_e) \quad (3)$$

$$\frac{C_e}{q_e} = \frac{1}{K_L q_m} + \frac{1}{q_m} C_e \quad (4)$$

Where C_e (mg/g) is the concentration of the Fe(III) at equilibrium, q_e (mg/g) is the equilibrium adsorption capacity of the Fe(III) adsorbed on the unit mass of the NaY zeolite, q_m (mg/g) is the maximum adsorption capacity, C_e (mg/L) is the concentration of the Fe(III) at equilibrium, K_F (L/mg) is the Freundlich adsorption equilibrium constant and K_L (L/mg) is the Langmuir adsorption equilibrium constant.

Figure 4 displays adsorption isotherm of Fe(III) tested at 30 °C, fitted by utilizing Freundlich and Langmiur isotherm models. The results indicated that the adsorption isotherm of Fe(III) solution was well fitted with both of those models according to correlation coefficient (R^2) approaching to 1. However, the adsorption of Fe(III) at 40 °C and 50 °C was only well respected with Freundlich model as shown in Table 1. Thus, the resulting suggested that the existence of adsorption phenomenon could be both physisorption and chemisorption. The initial adsorption was monolayer chemisorption, occurring rapidly on an abundant silanol group (-OH) in NaY. The adsorption rate decreased because the silanol group (-OH) in NaY reduced resulting from a lower electrostatic interaction. Then, a weaker adsorption, physisorption was dominant and likely released by the higher heating and energy (Sharififard et al., 2016; Artkla Choi, & Wittayakun, 2009).

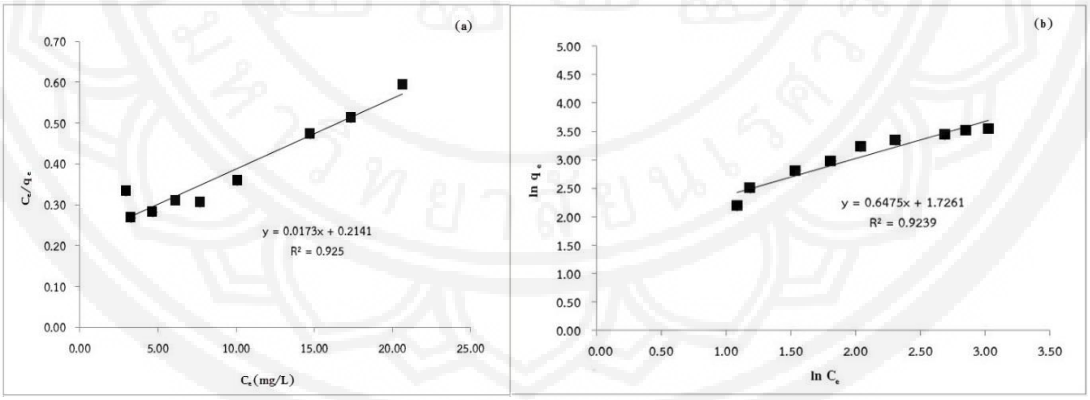

Figure 4 Adsorption isotherm of Fe(III) at 30 °C; Langmuir (a) and Freundlich (b)

Table 1 Parameters of Fe(III) adsorption isotherms.

Temperature (°C)	Langmuir isotherm			Freundlich isotherm		
	q_m (mg/g)	K_L (L/mg)	R^2	K_F (L/g)	n	R^2
30	57.80	0.0808	0.9250	0.5458	1.5444	0.9239
40	90.91	0.0514	0.7853	0.7389	1.2799	0.9553
50	60.61	0.5204	0.8790	1.0982	1.7892	0.9485

Kinetic absorption study

The influence of various concentrations from 20.00-100.00 (mg/L) on kinetic adsorption was studied. Moreover, pseudo-first order and pseudo-second order were employed to predict a kinetic adsorption behavior as displayed in equations 5 and 6, respectively.

$$\ln(q_e - q_t) = \ln q_e - k_1 t \quad (5)$$

$$\frac{t}{q_t} = \frac{1}{k_2 q_e^2} + \frac{1}{q_e} t \quad (6)$$

Where q_e (mg/g) is the equilibrium adsorption capacity of Fe (III) adsorbed on unit mass of NaY zeolite, q_t (mg/g) is the amount of Fe(III) adsorbed at time t, k_1 is the rate constant of pseudo-first order model and k_2 is the rate constant of pseudo-second order.

Figure 5 and Table 2 disclose models of Fe(III) absorption; pseudo-first order and pseudo-second order modes. The adsorption nature of Fe(III) was well correlated with pseudo-second order model due to correlation coefficient (R^2) value, closing to 1. In addition, the amount of adsorbed Fe(III) at equilibrium obtained from the calculation was nearly similar to that from experiment using pseudo-second order model. The results indicated that the adsorption of Fe species could be achieved rapidly by the diffusion into the porous, a rate limiting step (Ren et al., 2016) and the possible interaction of Fe adsorbed on NaY was Fe-NaY.

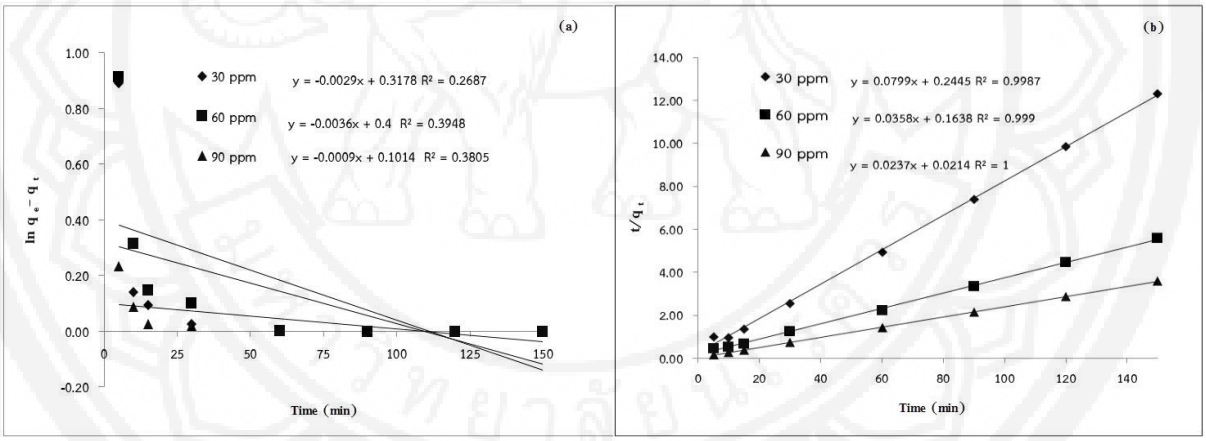

Figure 5 Model of Fe(III) absorption; pseudo-first order (a) and pseudo-second order model (b).

Table 2 Parameters of kinetic Fe(III) absorption

Concentration (mg/L)	$q_{e,exp}$ (mg/g)	Pseudo-first order			Pseudo-second order		
		k_1 (min^{-1})	$q_{e,cal}$ (mg/g)	R^2	k_2 (g/mg min)	$q_{e,cal}$ (mg/g)	R^2
30	16.02	0.0029	1.3741	0.2687	0.0261	20.08	0.9987
60	26.76	0.0036	1.4918	0.3948	0.0078	27.39	0.9990
90	41.76	0.0009	1.1067	0.3805	0.0262	45.04	1.0000

Thermodynamic study

The effect of various temperatures on the equilibrium state for thermodynamic values was calculated based on the Van't Hoff equations as shown in equations 7 and 8 to find out enthalpy change ($\Delta H°$), the entropy change ($\Delta S°$) and Gibbs free energy change ($\Delta G°$).

$$\Delta G^{o} = -RT \ln K_c \quad (7)$$

$$\ln K_c = \frac{\Delta S^{\circ}}{R} - \frac{\Delta H^{\circ}}{RT} \quad (8)$$

Where K_c is the constant value, T(K) is the absolute temperature and R is the universal gas constant (8.319 J/molK).

Figure 6 demonstrates the changes of enthalpy ($\Delta H°$) and entropy ($\Delta S°$) calculated from the equation of Van't Hoff equations. The changes of enthalpy ($\Delta H°$) and entropy ($\Delta S°$) for the adsorption processes were obtained from the intercept and slope plotting between $\ln K_c$ and 1/T. Table 3 presents the positive values of $\Delta H°$ and $\Delta S°$ and the negative value of $\Delta G°$. The positive values of $\Delta H°$ indicated that the adsorption process of Fe(III) was endothermic because the adsorption rate enlarged with increasing the temperature. The positive value of $\Delta S°$ suggested that some structural changes occurred on the NaY zeolite and the randomness between the solid and liquid interface enhanced during the adsorption process (He et al., 2010). Moreover, the negative value of $\Delta G°$ confirmed that the nature of adsorption process was spontaneous and more favorable at higher temperatures due to the lower negative of $\Delta G°$. Figure 7 exhibits the correlation between the potential and the activation energies of Fe(III) adsorption on NaY zeolite to distinguish the types of adsorption, chemical and/or physical adsorption. Faust and Aly (1987) reported that the values of $\Delta H°$ ranged from 83 to 420 (kJ/mol) were considered as a chemical absorption process. In addition, Wu (2007) reported that the value of $\Delta H°$ was lower than 40 (kJ/mol), considered as the physical absorption. Therefore, the value of $\Delta H°$ for Fe(III) adsorption on NaY in this work, 76.36 (kJ/mol) was the chemical absorption rather than physical absorption. The concluding remark was consistent with the result from isotherm study.

Table 3 Parameters on Fe(III) adsorption for thermodynamic study

Temperature (K)	$\Delta G°$ **(KJ/mol)**	$\Delta H°$ **(KJ/mol)**	$\Delta S°$ **(J/mol·K)**
303.15	-3.57		
313.15	-5.93	76.36	263.40
323.15	-8.85		

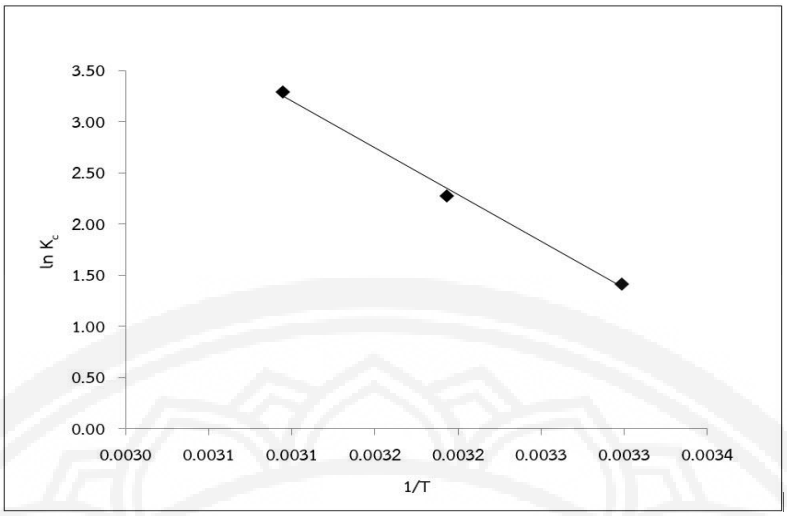

Figure 6 The changes of enthalpy ($\Delta H°$) and the entropy ($\Delta S°$) plotted between $\ln K_c$ and 1/T (NaY 0.1 g, 30 - 50 °C, pH = 5 and measured at 30 min)

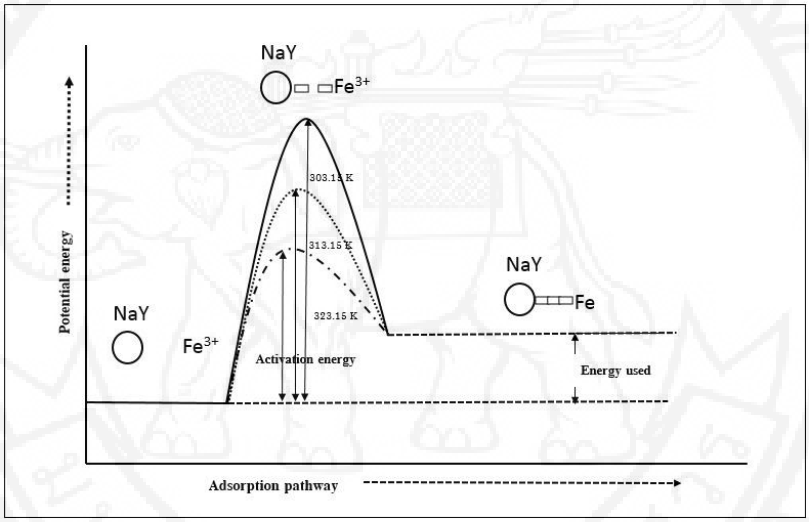

Figure 7 Correlation between the potential and the activation energies of Fe(III) adsorption on NaY zeolite (scale used for comparison)

Conclusions

The adsorption of Fe(III) from aqueous solution by the NaY zeolite synthesized from rice husk was studied. The NaY zeolite could be used as an adsorbent on Fe(III) adsorption at various optimized conditions including contact time, initial concentration, amount of NaY zeolite, pH of Fe(III) solution and temperature. The suitable contact time and amount of the NaY zeolite were 30 minutes and 0.10 g leading to equilibrium. The optimum pH on the Fe(III) adsorption was in the range of 4.0 to 6.0 because there was a lower of the competitive adsorption between H^+ and Fe(III) at lower pH and precipitation of Fe(III) at higher pH. Moreover, adsorption capacity of Fe(III) solution improved with increasing the temperature and initial concentration. The adsorption isotherm of the Fe(III) tested at 30 °C was well fitted with Langmuir model but that of Fe(III) tested at 40 °C and 50 °C were likely correlated to the Freundlich model indicating the existence both of chemical and physical adsorptions processes. The presence of positive enthalpy ($\Delta H°$) and entropy ($\Delta S°$) suggested the adsorption process of Fe(III) was an endothermic and disordered system. The

value of ΔH° on Fe(III) adsorption, 76.36 (kJ/mol) was inclined as the chemical absorption. Furthermore, the appearance of negative Gibbs free energy (ΔG°) indicated that adsorption process of Fe(III) was spontaneous and more favorable at higher temperatures due to the presence of the lower negative values of ΔG°. Finally, the kinetic adsorption of Fe(III) on NaY zeolite was well respected with the pseudo-second order model.

Acknowledgements

The research team would acknowledge the Program of Chemistry, Faculty of Science and Technology, Nakhon Ratchasima Rajabhat University, Thailand. Thanks also to Mr. Roy I. Morien of the Naresuan University Graduate School for his assistance in editing this paper to ensure correct English grammar and English expression.

References

Artkla, S., Choi, W., & Wittayakun, J., (2009). Enhancement of catalytic performance of MCM-41 synthesized with rice husk silica by addition of titanium dioxide for photodegradation of alachlor. *Environment Asia, 1*, 41-48.

Brook, M. A., Castle, L., Smith, J. R. L., Higgins, R., & Morris, K. P. (1982). Aromatic hydroxylation, part 7, oxidation of some benzenoid compounds by iron compounds and hydrogen peroxide with the aromatic compound acting as substrate and solvent. *Journal of the American Chemical Society, Perkin Transactions 2,* 687-692.

Bunmai, K., Osakoo, N., Deekamwong, K., Rongchapo, W., Keawkumay C., Chanlek, N., Prayoonpokarach, S., & Wittayakun, J. (2018). Extraction of silica from cogon grass and utilization for synthesis of zeolite NaY by conventional and microwave-assisted hydrothermal methods. *Journal of the Taiwan Institute of Chemical Engineers*, *83*, 152-158.

Choi, J. S., Yoon, S. S., Jang, S. H., & Ahn, W. S., (2006). Phenol hydroxylation using Fe-MCM-41 catalysts. *Catalysis Today*, *111*(3-4), 280-287.

Deng, R., Hu, Y., Ku, J., Zuo, W., & Yang, Z. (2017). Adsorption of Fe(III) on smithsonite surfaces and implications for flotation. *Colloids and Surfaces A: Physicochemical and Engineering Aspects, 533*, 308-315.

Faust, S. D., & Aly, O. M. (1987). *Adsorption process for water treatment*. Butterworths Publishers: Stoneham.

Ginter, D. M., Bell, A. T., & Radke, C. J. (1992). The effects of gel aging on the synthesis of NaY zeolite from colloidal silica. Zeolites. *12*(6), 742-749.

Hashemian, S., Hosseini, S. H., Salehifar, H., & Salari, K. (2013). Adsorption of Fe(III) from aqueous solution by Linde Type-A zeolite. *American Journal of Analytical Chemistry, 4*, 123-126.

He, J., Hong, S., Zhang, L., Gan, F., & Ho, Y.S. (2010). Equilibrium and thermodynamic parameters of adsorption of methylene blue onto rectorite. *Fresenius Environmental Bulletin*, *19*(11a.), 2651-2656.

Johar, N., Ahmad, I., & Dufresne, A. (2012). Extraction, preparation and characterization of cellulose fibres and nanocrystals from rice husk. *Industrial Crops and Products*, *37*(1), 93-99.

Khemtong, P., Prayoonpokarach, S., & Wittayakun, J. (2007). Synthesis and Characterization of Zeolite LSX from Rice Husk Silica. *Suranaree Journal Science Technology*, *14*(4), 367-379.

Kosri, C., Deekamwong, K., Sophiphun, O., Osakoo, N., Chanlek, N., Karin, F., & Wittayakun, J. (2017). Comparison of Fe/HBEA catalysts from incipient wetness impregnation with various loading on phenol hydroxylation. *Reaction Kinetics, Mechanisms and Catalysis*, *121*, 751-761.

Kulawong, J., & Kulawong, S. (2017, 8-11 February). Phenol adsorption on zeolite NaY synthesized from rice husk silica. *12th International workshop for east asian young rheologists*, Thailand: Chonburi.

Kulawong, S., Prayoonpokarach, S., Neramittagapong, A., & Wittayakun, J. (2011). Mordenite modification and utilization as supports for iron catalyst in phenol hydroxylation. *Journal of Industrial and Engineering Chemistry*, *17*(2), 346-351.

Mäki-Arvela, P., & Murzin D.Y. (2013) Effect of catalyst synthesis parameters on the metal particle size. *Applied Catalysis A: General. 451*, 251-281.

Osakoo, N., Pansakdanon, C., Sosa, N., Deekamwong, K., Keawkumay C., Rongchapo, W., ... Wittayakun, J. (2017). Characterization and comprehension of zeolite NaY/mesoporous SBA-15 composite as adsorbent for paraquat. *Materials Chemistry and Physics*, *193*(1), 470-476.

Park, J. N., Wang, J., Choi, K. Y., Dong, W. Y., Hong, S. I., & Lee, C. W., (2006). Hydroxylation of Phenol with H_2O_2 over Fe^{2+} and/or Co^{2+} Ion-exchanged NaY Catalyst in the Fixed-bed Flow Reactor. *Journal of Molecular Catalysis A: Chemical*, *247*(1-2), 73-79.

Preethi, M. E. L., Revathi, S., Sivakumar, T., Manikandan, D., Divakar, D., Rupa, A. V., & Palanichami, M. (2008). Phenol hydroxylation using Fe/Al-MCM-41 catalysts. *Catalysis Letters*, *120*(1-2), 56-64.

Rakmae, S., Keawkumay, C., Osakoo, N., Montalbo, K. D., de Leon, R. L., Kidkhunthod, P., ... Wittayakun, J. (2016) Realization of active species in potassium catalysts on zeolite NaY prepared by ultrasound-assisted impregnation with acetate buffer and improved performance in transesterification of palm oil. *Fuel*, *184*, 512-517.

Real, C., Alcala, M. D., & Criado, J. M. (1996) Preparation of Silica from Rice Husks. *Journal of the American Ceramic Society*, *79*(8), 2012-2016.

Ren, H., Gao, Z., Wu, D., Jiang, J., Sun, Y., & Luo, C. (2016). Efficient Pb(II) removal using sodium alginate-carboxymethyl cellulose gel beads: Preparation, characterization, and adsorption mechanism. *Carbohydrate Polymers*, *137*, 402-409.

Seliem, M. K., & Komarneni, S. (2016) Equilibrium and kinetic studies for adsorption of iron from aqueous solution by synthetic Na-A zeolites: Statistical modeling and optimization. *Microporous and Mesoporous Materials*, *228*, 266-274.

Sharififard, H., Pepe, F., Soleimani, M., Aprea, P., & Caputo, D. (2016) Iron-activated carbon nanocomposite: synthesis, characterization and application for lead removal from aqueous solution. *RSC Advances*, *6*, 42845-42853.

Villa, A. L., Caro, C. A., & de Correa, C. M. (2005). Cu- and Fe-ZSM-5 as Catalysts for Phenol Hydroxylation. *Journal of Molecular Catalysis A: Chemical*, *228*(1-2), 233-240.

Wang, L., Zhang, J., Zhao, R., Li, Y., & Zhang, C. (2010). Adsorption of Pb(II) on activated carbonprepared from Polygonumorientale Linn. : Kinetics, isotherms, pH, and ionic strength studies. *Bioresource Technology, 101*(15), 5808-5814.

Wantala, K., Sthiannopkao, S., Srinameb, B., Grisdanurak, N., & Kim, K. W., (2010). Synthesis and characterization of Fe-MCM-41 from rice husk silica by hydrothermal technique for arsenate adsorption. *Environ Geochem Health, 32*(4), 261-266.

Wittayakun, J., & Grisdanurak, N., (2004). Catalysis: *Fundamentals and Applications*. Bangkok: Thammasat Printing house.

Wittayakun, J., Khemthong, P., & Prayoonpokarach, S., (2008) Synthesis and characterization of zeolite NaY from rice husk silica. *Korean Journal of Chemical Engineering, 25*(4), 861-864.

Wu, C. H., (2007). Adsorption of reactive dye onto carbon nanotubes: Equilibrium, kinetics and thermodynamics. *Journal of Hazardous Materials, 144*(1-2), 93-100.

Zhao, W., Luo, Y., Deng, P., & Li, Q., (2001). Synthesis of Fe-MCM-48 and Its Catalytic Performance in Phenol Hydroxylation. *Catalysis Letters, 73*(2-4), 199-202.